An Optimized Design of Solar Burner Through Thermal and Structural Analysis of Plate and Coil of Burner using ANSYS.

Syed Asfandyar, M.S.[1], Muhammad Rafique, Ph.D.[2*], and M. Javed Hyder, Ph.D.[3]

[1]C-2 Project, Pakistan Atomic Energy Commission, Islamabad, Pakistan.
[2]Department of Physics, University of Azad Jammu & Kashmir,
Post Office Muzaffarabad 13100, Azad, Kashmir.
[3]Department of Chemical and Mechanical Engineering, PIEAS,
Post Office Nilore, Islamabad 45650, Pakistan.

[*]E-mail: mrafique @gmail.com
Rafi_722002@yahoo.com
Fac014@pieas.edu.pk

ABSTRACT

This paper presents an optimized design of a solar burner using the finite element package ANSYS®. Due to high conduction properties, copper metal has been used for both the coil and plate. The1.22 W pump power has been required for circulating oil in the circuit. Different cases for thermal and structural analysis of the plate and coil have been used in varying thickness of the plate for both in the case of heat removal and in the absence of heat removal. In each case, the temperature of the oil at the coil inlet has been taken as 270 C.

In absence of heat removal of 30kW/m^2 the oil leaves the coil at 165 C while in the case of heat removal the oil leaves at a temperature of 144.3 C. In absence of heat removal the deformation produced in 5 mm, 1 cm, 1.5 cm and 2 cm thick plates have been observed as 0.859 mm, 0.472 mm, 0.3 mm and 0.223 mm, respectively. The Von Mises stresses observed are 557 MPa, 546 MPa and 536 MPa for 5 mm, 1 cm, 1.5 cm and 2 cm thickness of the plate, respectively.

In the case of heat removal, the deformation in 2mm, 5 mm, and 1 cm thick plates come out to be 0.0682 mm, 0.086 mm and 0.138 mm, respectively. The Von Mises stresses for these thicknesses are 561 MPa, 487 MPa, and 477 MPa, respectively. The optimum plate thickness is found to be 5 mm. It is best suited for use in the burner from a thermal as well as structural point of view.

(Keywords: ANSYS®, optimized design, solar burner, structural analysis, Von Mises stresses)

INTRODUCTION

Sunlight or solar energy can be used to generate electricity, provide hot water, and to heat, cool, and light buildings [1]. A power plant can use a concentrating solar power system, which uses the sun's heat to generate electricity. The sunlight is collected and focused with mirrors to create a high-intensity heat source. This heat source produces steam or mechanical power to run a generator that creates electricity.

Solar water heating systems for buildings have been developed. Many large commercial buildings can use solar collectors to provide more than just hot water. Solar process heating systems can be used to heat these buildings. A solar ventilation system can also be used in cold climates to preheat air as it enters a building. Additionally, the heat from a solar collector can even be used to provide energy for cooling a building.

Day lighting is simply the use of natural sunlight to brighten up a building's interior. Many scientists and engineers directed their efforts towards utilization of solar energy to generate electricity, provide hot water, and to heat, cool, and light buildings in different parts of world [2-17].

The purpose of this paper is to design a solar burner for the household purposes. Solar Burners can be used for cooking as well as heating rooms where the conventional means of heating are not available easily, for example in deserts and in dry hilly areas where coal, wood, oil, and natural gas

are not easily available. Furthermore most of the time the weather in Pakistan is sunny and normally the sky is clear so the energy flux coming from the Sun is normally high enough to make the existence of the solar technology feasible. In the current study, transformer oil (T300) was considered as a working fluid because it does not boil at a temperature of 270 C and its flash point is nearly 550^0F (288 C) [18]. This oil is basically used in transformers and in high speed racing cars and is intended for use where extremely high temperatures may be encountered and when engine durability is the primary concern. Another option for use as heat transfer oil is SAE 70 oil, which also remains liquid at very high temperatures, and is more highly viscous oil than SAE 50 or other engine oils. Water is not feasible for use as a heat transfer medium because of its low boiling point as well as its corrosive property.

MATHEMATICAL CALCULATIONS

Calculations for pump power, convective heat transfer coefficient (h), thermal stresses, and deformation due to thermal stresses and heat flux have been carried out below:

Calculations for Pump Power

From the Figure 1, the dimensions of the systems have been taken as:

Length of the flow circuit = 17.5 m
Datum head = $Z_2 - Z_1$ = 5m

Fittings:

½" (90^0) Elbows = 6
½" Tees = 2
½" Gate Valves = 2

Tube diameter = d = 1cm
Velocity of oil = V = 0.2 m/s (assumed)
Viscosity = v= 5.6 * 10^{-6} m^2 /s [1].

Applying Bernoulli's Equation between section 1 and 2, [20]:

$$\frac{p_1 - p_2}{\rho g} + \frac{V_1^2 - V_2^2}{2g} + h_p = Z_2 - Z_1 + h_f + \sum h_m \qquad \textbf{(1)}$$

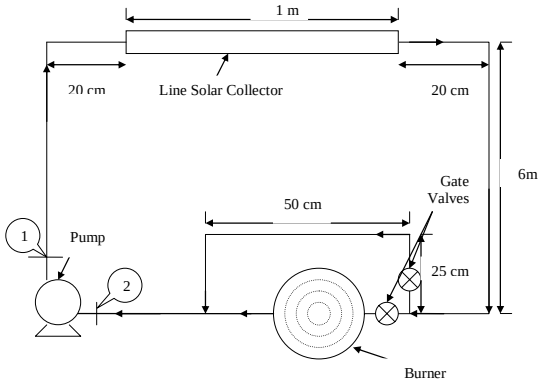

Figure 1: Schematic Diagram for the Solar Burner Setup. *Review Stage.*

where:

p_1, p_2 : pressures at pump inlet and outlet respectively
V_1 ,V_2 : Velocities at pump inlet and outlet respectively
Z_1,Z_2 : Datum Heads
ρ: Density of Oil
h_p : Pump Head
h_f : major (friction) losses
Σh_m : Minor Losses.

As $p_1 = p_2$ and $V_1 = V_2$ (assuming no pressure drop in pump), so the refined equation becomes:

$$h_P = Z_2 - Z_1 + h_f + \Sigma h_m \qquad \textbf{(2)}$$

$$\Rightarrow h_p = Z_2 - Z_1 + \frac{V^2}{2g}\left(\frac{fL}{d} + \sum K\right) \qquad \textbf{(3)}$$

Now the minor loss Coefficient is given by,

Σ K = 6* 2 +3.3*2 + 0.3*2 = 19.2

as $R_e = \frac{Vd}{\nu}$ = 0.2* 0.01/5.6*10^{-6} = 357.14 < 2300

so the flow is highly Laminar. So f = 64/R_e = 0.18

Putting values in the equation we get,

$$h_p = 5 + \frac{0.2^2}{2*9.8}\left(\frac{0.18*17.5}{0.01} + 19.2\right)$$

$$\Rightarrow h_p = 5.68m$$

Now as pump power is given by, [20]

$$P = \rho g h_P Q \qquad \textbf{(4)}$$

Here Q = AV = $\pi d^2/4 * 0.2$

Q = $1.57 * 10^{-5}$ m^3/S

So the equation becomes, P = 0.79 W.

Let the pump efficiency be η = 65%,
Then P = 0.79/0.65 = 1.22 W.

Calculations for Convective Heat Transfer Coefficient (h)

For oil, k=0.132 W/m.K
R_e = 357.14 << 2300

As the flow is highly laminar the Nusselt No. will become constant [21].

Nu = 4.364

As Nu = hd/k **(5)**

So, h= 4.364*0.132/0.01
h= 57.6 $W/m^2.K$

where,
k: Thermal Conductivity
Re: Reynold's No.
Nu: Nusselt No.

Calculations for Thermal Stresses and Deformation due to Thermal Stresses

For the plate thickness = 5mm
As thermal stresses in the plate are given by [22].

$$\sigma = -E\alpha T \qquad \textbf{(6)}$$

(Negative sign indicates compressive stress with increase in temperature.)

For copper [23]:

E = 117 GPa
α = $1.66*10^{-5}$ C^{-1}
υ = 0.3
Now T = 270 ^{0}C

So the equation gives the value of thermal stress is expressed as,

σ = -524.4 MPa,

and deformation is given by,

$$\delta = \frac{\alpha D T}{2(1-\upsilon)} \qquad \textbf{(7)}$$

Now as D = 0.32m
So δ = 0.716 mm

Where:
α: Linear Coefficient of Thermal Expansion
E: Modulus of Elasticity
σ: Thermal Stress
ν: Poisson Ration
δ: Deformation

Calculations for Heat Flux

As the upper half area of the solar collector is exposed to solar radiation, the thermal flux for the coil is calculated as:

Dimensions of the collector:
Length of Collector = L = 3m
Diameter of the Collector = D = 0.015 m

So total surface area of the collector = A = π DL = 0.1414 m^2.

As half of the area of the collector is exposed to solar radiation through the concentrator, so

Effective area of the collector = A_{eff} = 0.1414/2 = 0.070 m^2

Thermal Flux falling on collector= 40 x 10^3 W/m^2

Total heat supplied to the collector = Q = 40 x 10^3 x .070 = 2800 W

Now for the coil,
Length of the coil = l = 2.5 m
Diameter of the coil = d = .01m

So total surface area of the coil = A_c = π d l = 0.07854 m^2

Assuming the one-third area of the coil is in contact with the plate through which conduction heat transfer takes place, so,

Effective area of the coil = A_{ceff} = 0.07854/3 = 0.0262 m^2

So heat flux removed from the coil = = 2800 / 0.0262 = 106870 w/m^2

Assuming a 30% conversion efficiency for the coil, heat flux obtained is as: Heat flux from the coil = 106870 x 0.3 = 32 x $10^3 \approx$ 30 x 10^3W/m^2

RESULTS AND DISCUSSIONS

Two cases for thermal and structural analysis of the plate and coil have been carried out by varying thickness of the plate for both the case of heat removal and in the absence of heat removal.

Without Heat Removal

The results obtained from the ANSYS® analyses (i.e. from thermal analysis of the coil and plate assembly and from the coupled thermal – structural analyses for plates with different thickness without heat removal from the plate) are shown in Figures 2 to 8.

In Figures 2 and 3, the temperature distribution in the coil and plate of 5mm thickness is given.

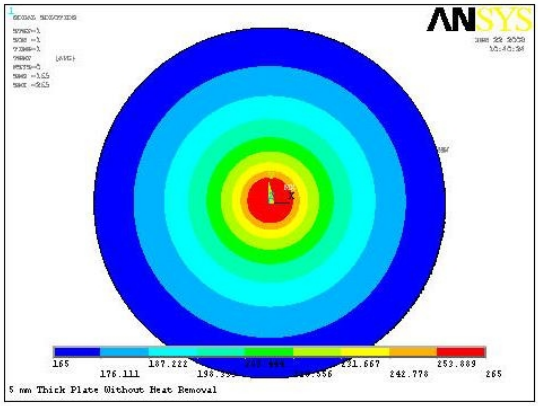

Figure 2: Temperature Distribution in the Plate (without heat removal).

From the Figures 2 and 3 it is clear that the oil enters into the coil at about 270 C and leaves at about a temperature of 165 C, in the case without heat removal, and at144.3 C with heat removal of 30kW/m^2.

The coil was arranged to make the flow outward. This arrangement was done to minimize the heat transfer losses to the environment and make efficient use of the heat energy carried by the oil. The velocity of the oil was kept 0.2 m/s, which is very low. The velocity of the oil was kept low to provide more time for heat transfer, thus enhancing heat transfer to the coil and plate.

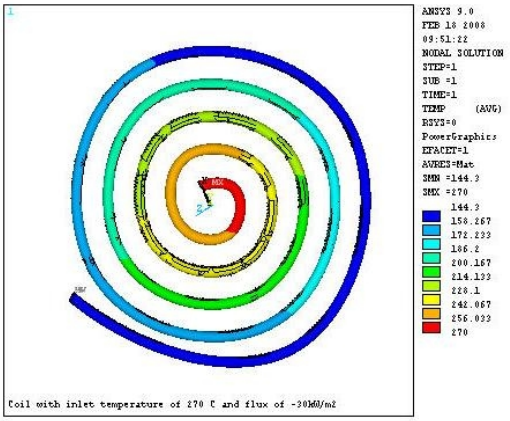

Figure 3: Temperature Distribution in the Coil (with heat removal).

The above temperature distribution was used in the coupled thermal-structural analysis of the plate for different thicknesses. The analysis was assumed as a static steady state problem so that the temperature distribution attained an asymptotic value.

The material selected for both coil and plate was copper due to its higher conduction properties. The deformation produced a plate of 5 mm thicknesses is shown in Figure 4.

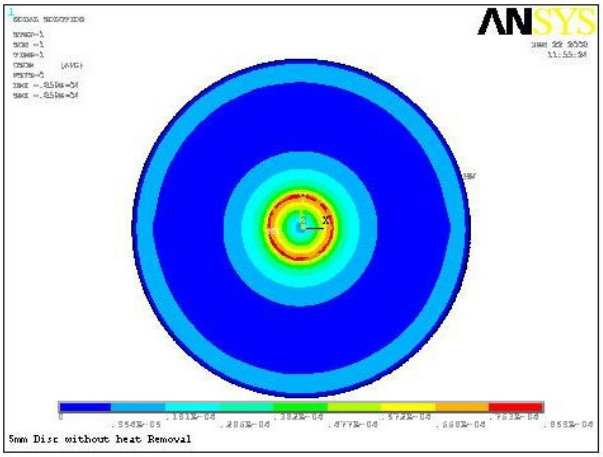

Figure 4: Total Deformation (in meters) for 5 mm Thick Plate.

Structural Analysis of Plate Deformation

The deformation in the plates with respective thicknesses are given in the Table 1. Form Table 1 it is clear that increasing the thickness of the plate reduces the buckling of the plate.

For the plate thickness of 2mm the maximum deformation of the plate is 2.11 mm while that for 5 mm, 1 cm, 1.5 cm and 2 cm plate the maximum deformation is 0.859 mm, 0.472 mm, 0.3mm, and 0.223 mm, respectively. A plot of plate thickness vs. maximum deformation of the plate is given in Figure 5.

Table 1: Table of Plate Deformation with its Thickness.

Thickness (mm)	Deformation (mm)
2	2.119
5	0.859
10	0.472
15	0.3
20	0.223

The plot shows that increasing the plate thickness the deformation approaches an asymptotic value. Beyond 2 cm, the deformation becomes almost constant.

As 0.859 mm deformation of the plate of 5mm thickness is an acceptable value because the deformation is so small that the contact between coil and plate due to plate deformation will not break except in a very small region at the center of the plate. Also reducing the plate thickness enhances the heat transfer properties so it seems the best-suited thickness for the plate to be used in the burner.

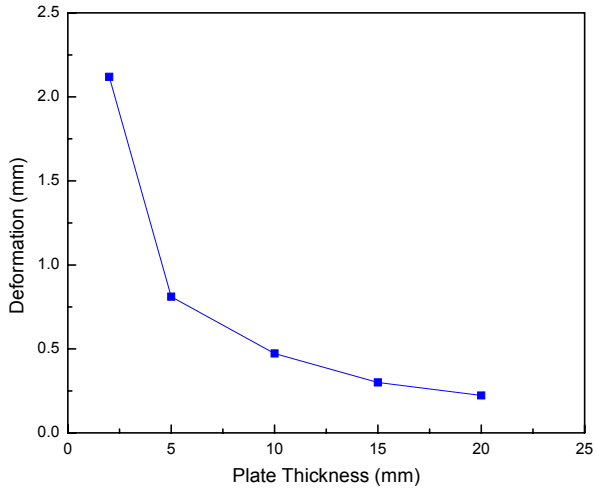

Figure 5: Plot of deformation Vs. Plate Thickness.

Stresses

From the results in Figure 7, it is clear that the Von Mises stresses are of decreasing stress levels with increasing plate thickness. Figure 6 indicates the Von Mises stress for the 5 mm plate is 557 MPa. Figure 7 shows the Von Mises stress for 1.5 cm thick plate as 546 MPa and for a 2 cm thick plate the stress is 536 MPa. The reason for this variation in stress levels is that as the thickness of the plate is increased, the projected area resisting to the compression increases, resulting in a reduction of the stress. Figure 7 shows a plot of variation of stress level in the plate with its thickness.

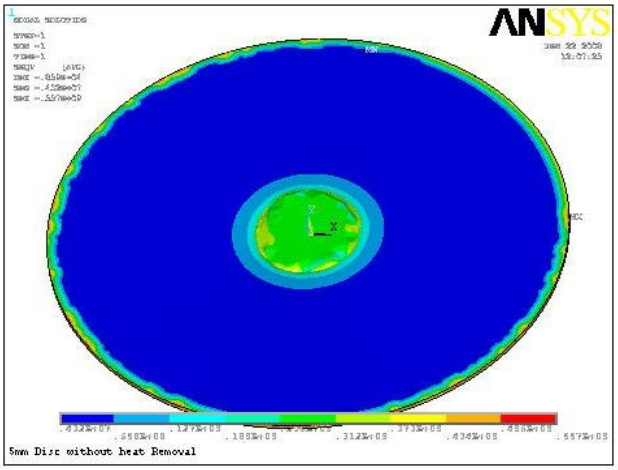

Figure 6: Von Mises Stresses on Back Side of the Plate (Pa) for 5 mm Thickness.

Tensile strength of the Electrolytic Copper is 383 MPa [23]. Also the compressive strength of the materials is usually double that of tensile strength, so the compressive strength of the copper is 766 MPa.

At the present stress levels, the shape of the plate having minimum thickness (i.e. 5 mm) will not distorted permanently and after cooling the plate (i.e. when the burner is not in use and the hot oil is passing through the bypass passage in the circuit), the plate will regain its original un-deformed shape. The deformation and various stresses in the plates of different thicknesses are shown in Table 2.

Table 2: Variation of Deformation and Stress Level with Plate Thickness.

S No.	Thickness (mm)	Deformation (mm)	Von Mises Stress (MPa)
1	2	2.119	665
2	5	0.859	557
3	10	0.472	556
4	15	0.30	546
5	20	0.223	536

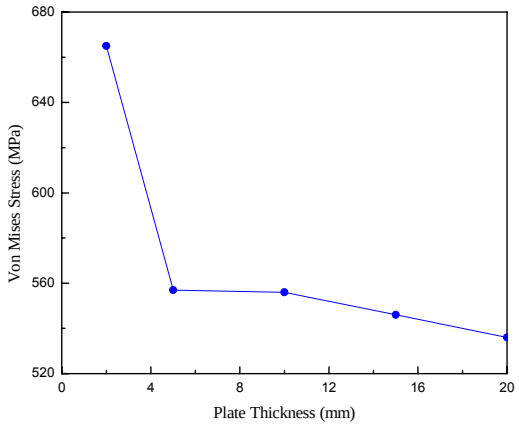

Figure 7: Variation of Stress Level with Plate Thickness.

With Heat Removal

As the oil passes through the coil it transfers heat to the coil and in turn to the plate, so negative heat flux is applied on the area the coil in contact with the plate and on the upper face of the plate. The value of the heat flux removed from the coil and plate is –30 kW/m^2. The negative sign indicates removal of the heat from the surface of the coil and plate the coil and plate were analyzed separately to see the temperature distribution in both components clearly.

The results obtained from the ANSYS® analyses (i.e. from thermal analysis of the coil and plate assembly and from the coupled thermal – structural analyses for plate with 5mm thickness with heat removal at a rate of –30 kW/m^2 from the plate) are shown below.

In Figure 8 the temperature distribution in the coil is shown. It is clear that the oil entered in the coil at 270 C, dissipating heat to the coil and leaves the coil at 144.3 C. It is indicated by Figure 8 that higher the temperature of the oil, the greater the heat transfer rate. The temperature drops initially very quickly which is a confirmation of Newton's law of cooling which states that the rate of heat transfer is directly proportional to the temperature difference between the hot and cold bodies. As the temperature of the oil decreases, the rate of heat transfer decreases and the drop rate of the oil temperature is retarded.

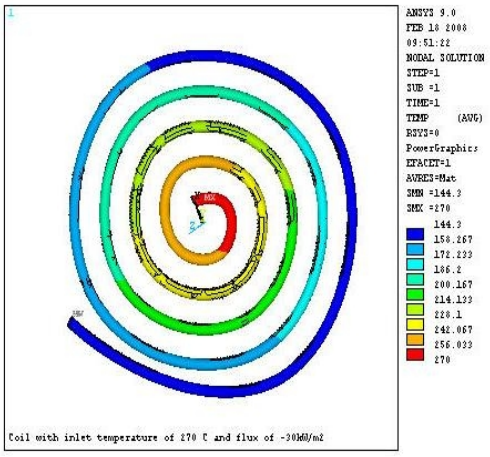

Figure 8: Temperature Distribution in the Coil with Heat flux of -30 kW/M$^{2.}$

Similarly, in Figure 9, temperature distribution in the plate of 5mm thickness is given. The maximum temperature is at the center of the plate (that is 265 C) while the minimum temperature is at the outer periphery of the plate (that is 144.3 C). It is revealed from Figures 5-9 that the greater the temperature of the oil, the greater the rate of heat transfer, and the temperature of the plate approaches the temperature of the coil. On the other hand, at the exit of the coil, the temperature of the oil is reduced affecting the heat transfer which causes a slight difference in the temperature of the coil and plate at the outer periphery.

Figure 10 shows the temperature distribution for a 1 cm thick plate. The maximum temperature is 270 C at the center of the plate, while the minimum temperature is 144.3 C at the outer periphery of the plate.

It is clear that with an increase in plate thickness the temperature drop in the plate is decreased, as shown from the comparison of Figures 9 and 10.

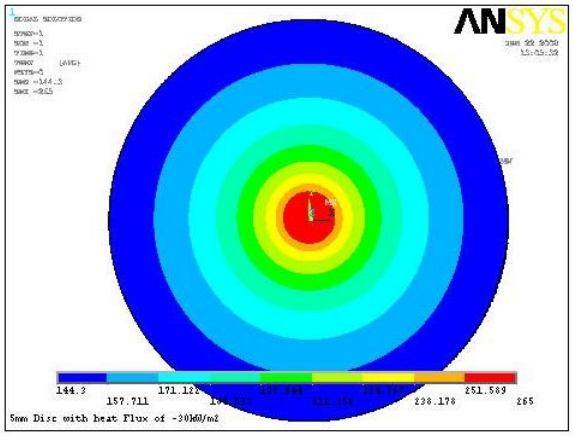

Figure 9: Temperature Distribution in 5mm Thick Plate with Heat Flux of -30 kW/m^2.

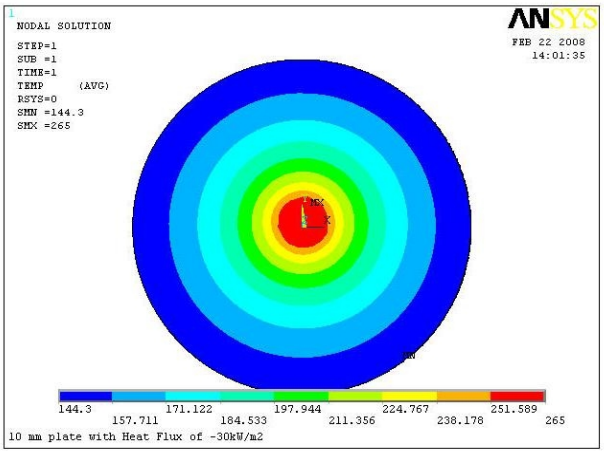

Figure 10: Temperature Distribution in 1 cm Plate with Heat Flux of -30 kW/m^2.

Structural Analysis of Plate Deformation

Form Figure 11 it is clear that with the application of negative heat flux (i.e. with the removal of heat from the plate) deformation in the plate decreases to a large extent. Figure 11 shows deformation for the plate thickness of 5mm. The maximum deformation in the plate is 0.086 mm, while that for a 2 mm and 1 cm plate, the maximum deformation is 0.0682 mm and 0.0641 mm, respectively as shown in Table 3.

From this table it is clear that with the removal of heat from the plate continuously decreases the deformation of the plate tremendously. The reason behind this reduction is that with the removal of heat, the plate temperature is maintained at a lower temperature as compared to that in case of without heat removal as cleared from the temperature distribution in both cases.

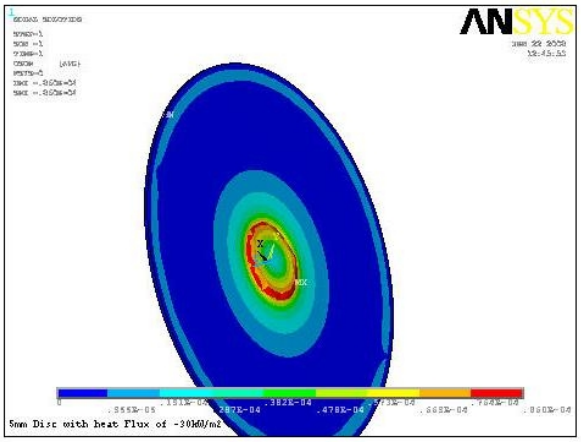

Figure 11: Deformation in 5 mm Thick plate with heat flux of -30 kW/m^2

Table 3: Deformation and Stresses in Plates with Respective Thicknesses.

S No.	Thickness (mm)	Deformation (mm)	S_{VM} (MPa)
1	2	.0682	449
2	5	0.086	487
3	10	.0641	531

Stresses

Figure 12 shows the Von Mises stress distribution in a 5 mm thick plate. It is clear from the figure that the stress level with the application of heat removal is decreased, but not changed too much, as in the case of deformation the Von Mises stress in 5 mm plate without heat removal (557 MPa). With heat removal it is 487 MPa. With respect to deformation, the application of heat removal for the same thickness plate results in a deformation decreases of about 10 times or more.

It is also clear from Table 4 that the stress level increases with increase in plate thickness. From Table 3, the Von Mises stress in a 1 cm thick plate is found to be 531 MPa which is more than that for the 2mm and 5 mm plates. The reason

for this increase is that with the increase in thickness of the plate, the temperature difference between the faces of the plate increases causing more stresses due to this thermal gradient. Variation of stresses with plate thickness with heat flux of -30 kW/m^2 is shown in Figure 13.

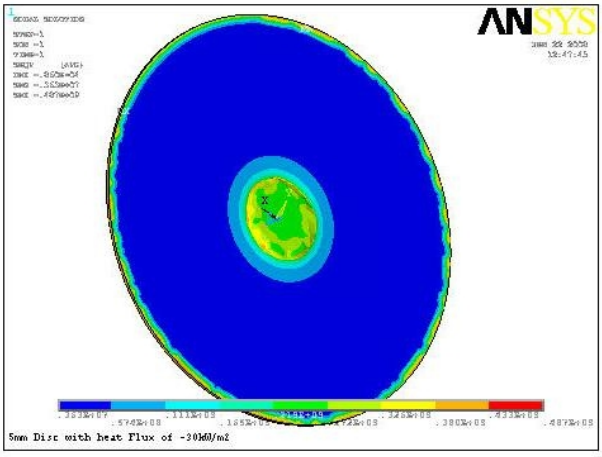

Figure 12: Von Mises Stress in 5 mm plate (MPa).

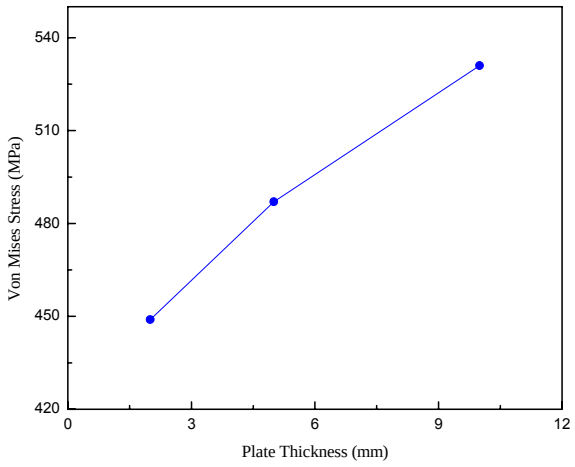

Figure 13: Variation of Stresses with Plate Thickness with Heat Flux of -30 kW/m^2.

ANSYS® VALIDITY

To check the ANSYS® validity for a particular analysis, the case of 5 mm thick plate was taken. The mathematical calculations for this thickness show the stress in the plate to be 524 MPa, while the ANSYS® shows the stress to be 557 MPa. Also, the deformation given by theoretical calculation show a deformation of 0.716 mm while ANSYS® show that maximum deformation in the plate is 0.859 mm. Thus the error between the analytical results and ANSYS® result is given as:

In deformation,

% Error = (0.859-0.716)*100/0.859

% Error = 16.65%

In thermal stress,

% Error = (592-524)*100 /592

% Error = 5.92%

CONCLUSION

From the results obtained from the analyses for plates of different thicknesses, it is clear that as the thickness of the plate is increased the deformation produced due to thermal stresses is decreased. From Figure 5-6 it is obvious that as the thickness of the plate is increased from 5mm to 1.5 cm, the deformation in the plate is drastically reduced, and beyond 1.5 cm the reduction in deformation with increasing thickness is retarded. Beyond 2 cm plate thickness, it approaches an asymptotic value beyond which there is no appreciable change in deformation with increasing plate thickness. So increasing plate thickness further would result no benefit in the sense of reduction in deformation. On the other hand it will result in a reduction in heat transfer, which will not be a desirable situation.

Further more if the thickness is reduced from 5 mm, the deformation as well as stress level will be increased causing the buckling of the plate which will break the contact between coil and the plate that will reduce the heat transfer. Also with the increase in stress level, the plate will be permanently deformed or yielded. So 5 mm is the optimum thickness for the plate to be used in burner both on the basis of heat transfer as well as structural rigidity point of view. Therefore, the final dimensions of the solar burner are as follows:

Material of the Coil and Plate: Copper
Length of the Coil: 2.5 m
Diameter of the Tube: 0.01m
Diameter of the Plate: 0.16 m
Thickness of the Plate: 0.005 m
Heat Transfer Fluid: T300 Oil (SAE70 Oil can also be used as an alternative).

ACKNOWLEDGMENTS

The authors acknowledge the enabling role of the Higher Education Commission, Islamabad, Pakistan and expresses their appreciation for its financial support through the Development of S&T Manpower through Indigenous Ph.D.

NOMENCLATURE

p_1, p_2 : pressures at pump inlet and outlet respectively
V_1 ,V_2 : Velocities at pump inlet and outlet respectively
Z_1, Z_2 : Datum Heads
ρ: Density of Oil
h_p: Pump Head
h_f : major (friction) losses
Σh_m : Minor Losses.
k: Thermal Conductivity
Re: Reynold's No.
Nu: Nusselt No.
α: Linear Coefficient of Thermal Expansion
E: Modulus of Elasticity
σ: Thermal Stress
ν: Poisson Ration
δ: Deformation
η: Efficiency

REFERENCES

1. Duffie, J.A. and Beckman. W.A. 1991. *Solar Engineering of Thermal Processes*. John Willey and Sons, Inc.: Singapore.

2. Oliveira, A.C., Afonso, C., Matos, J., Riffat, S., Nguyen, M., and Doherty, P. 2002. "A Combined Heat and Power System for Buildings Driven by Solar Energy and Gas". *Applied Thermal Engineering.* 22(6):587-593.

3. Lambert, M.A. 2007. "Design of Solar Powered Adsorption Heat Pump with Ice Storage". *Applied Thermal Engineering*. 27(8-9):1612-1628.

4. Colangelo, G., De Risi, A., and Laforgia, D. 2006. "Experimental Study of a Burner with High Temperature Heat Recovery System for TPV Applications". *Energy Conversion and Management*. 47(9-10):1192-1206.

5. Qiu, K. and Hayden, A.C.S. 2006. "Development of a Silicon Concentrator Solar Cell Based TPV Power System". *Energy Conversion and Management*. 47(4):365-376.

6. Kongtragool, B. and Wongwises, S. 2007. "Performance of a Twin Power Piston Low Temperature Differential Stirling Engine Powered by a Solar Simulator". *Solar Energy*. 81(7):884-895.

7. Palmero-Marrero, A.I. and Oliveira, A.C. 2006. "Evaluation of a Solar Thermal System using Building Louvre Shading Devices". *Solar Energy*. 80(5):545-554.

8. Thür, A., Furbo, S., and Jivan Shah, L. 2006. "Energy Savings for Solar Heating Systems". *Solar Energy* . 80(11):1463-1474.

9. Martinez, P.J., Velázquez, A,, and Viedma, A 2005. "Performance Analysis of a Solar Energy Driven Heating System". *Energy and Buildings.* 37(10):1028-1034.

10. Jubran, B.A., Al-Saad, M.A., and Abu-Faris, N. 1994. "Computational Evaluation of Solar Heating Systems using Concrete Solar Collectors". *Energy Conversion and Management.* 35(12):1143-1155.

11. Mills, D. 2004. "Advances in Solar Thermal Electricity Technology". *Solar Energy*. 76(1-3)19-31.

12. Fiedler, F., Nordlander, S., Persson, T., and Bales, C. 2006. *Renewable Energy*. 31(1):73-88.

13. Fiedler, F. 2004. "The State of the Art of Small-Scale Pellet-Based Heating Systems and Relevant Regulations in Sweden, Austria, and Germany". *Renewable and Sustainable Energy Reviews*. 8(3):201-221.

14. Srinivasan, S. 2006. "Transforming Solar Thermal Policy Support for the Evolving Solar Water Heating Industry. *Refocus*. 7(2):46-49.

15. Li, J. and Hu, R. 2005. "Solar Thermal in China: Overview and Perspectives of the Chinese Solar Thermal Market". *Refocus*. 6(5):25-27.

16. Nandi, P. and De, R. 2007. "Production of Sweetmeat Utilising Solar Thermal Energy: Economic and Thermal Analysis of a Case Study". *Journal of Cleaner Production*. 15(4):373-377.

17. Manrique, J.A. 1984. "A Compound Parabolic Concentrator". *International Communications in Heat and Mass Transfer*. 11(3):267-273.

18. Gupta, J.B. 1992. *Theory and Performance of Electrical Machines*. S.K Kataria & Sons: Delhi, India.

19. ANSYS Help Manual. 2006. *Basic Analysis Procedure Guide*. Parametric Technology Corporation: Needham, MA.

20. White, F.M. 1994. *Fluid Mechanics*. Mc Graw Hill: Singapore.

21. Holman, J.P. 2001. *Heat Transfer*. Mc Graw Hill: New York, NY.

22. Timoshenko, S. and Goodier, J.N. 1934. *Theory of Elasticity*. Mc Graw Hill: New Yok, NY.

23. Shigley, J.E. 1997. *Mechanical Engineering Design*. McGraw Hill: New York, NY.

ABOUT THE AUTHORS

Syed Asfandyar earned a Bachelor of Engineering from UET Peshawar and then a MS Nuclear Engineering from PIEAS.

Muhammad Rafique earned a M.Sc. in Physics from Azad Jammu & Kashmir University in 1997. He joined the Department of Physics, University of Azad Jammu & Kashmir in the year 1999 as a lecturer. In 2001, he joined Department of Physics & Applied Mathematics at Pakistan Institute of Engineering & Applied Sciences to pursue his Ph.D. studies. He completed his Ph.D. in 2005, and joined again the Department of Physics at the University of Azad Jammu & Kashmir. Currently he is serving as an Assistant Professor at the Department of Physics UAJ&K. His area of research is Reactor Physics, Radiation Shielding, and Fluid Dynamics. He has authored, several international and national research papers.

Mohammad Javed Hyder is serving as a Dean, Faculty of Engineering and Head, Department of Mechanical Engineering at Pakistan Institute of Engineering & Applied Sciences. He did his Ph.D. in Mechanical Engineering from Rensselear Polytechnic Institute. His Research Interests are Computational Engineering, Creep Fatigue Interaction, Computer Software Development, Finite Element Analysis, Applications of Computer Graphics in Engineering, and Turbo Machinery. He has authored, several international and national research papers.

SUGGESTED CITATION

Asfandyar, S., M. Rafique, and M.J. Hyder. 2008. “An Optimized Design of Solar Burner through Thermal and Structural Analysis of Plate and Coil of Burner using ANSYS”. *Pacific Journal of Science and Technology*. 9(1):132-141.